Biochimica et Biophysica Acta 1850 (2015) 1099–1106

Contents lists available at ScienceDirect

Biochimica et Biophysica Acta

journal homepage: www.elsevier.com/locate/bbagen

Investigation of the heparin–thrombin interaction by dynamic force spectroscopy

Congzhou Wang [a], Yingzi Jin [b], Umesh R. Desai [b], Vamsi K. Yadavalli [a,*]

[a] Department of Chemical and Life Science Engineering, Virginia Commonwealth University, Richmond VA 23284, United States
[b] Department of Medicinal Chemistry, Institute for Structural Biology and Drug Discovery, Virginia Commonwealth University, Richmond, VA 23298, United States

ARTICLE INFO

Article history:
Received 14 October 2014
Received in revised form 8 January 2015
Accepted 25 January 2015
Available online 31 January 2015

Keywords:
Heparin
Thrombin
Self-assembled monolayers
Atomic force microscopy
Force spectroscopy

ABSTRACT

Background: The interaction between heparin and thrombin is a vital step in the blood (anti)coagulation process. Unraveling the molecular basis of the interactions is therefore extremely important in understanding the mechanisms of this complex biological process.
Methods: In this study, we use a combination of an efficient thiolation chemistry of heparin, a self-assembled monolayer-based single molecule platform, and a dynamic force spectroscopy to provide new insights into the heparin–thrombin interaction from an energy viewpoint at the molecular scale.
Results: Well-separated single molecules of heparin covalently attached to mixed self-assembled monolayers are demonstrated, whereby interaction forces with thrombin can be measured via atomic force microscopy-based spectroscopy. Further these interactions are studied at different loading rates and salt concentrations to directly obtain kinetic parameters.
Conclusions: An increase in the loading rate shows a higher interaction force between the heparin and thrombin, which can be directly linked to the kinetic dissociation rate constant (k_{off}). The stability of the heparin/thrombin complex decreased with increasing NaCl concentration such that the off-rate was found to be driven primarily by non-ionic forces.
General significance: These results contribute to understanding the role of specific and nonspecific forces that drive heparin–thrombin interactions under applied force or flow conditions.

1. Introduction

Pair-wise biomolecular interactions involving different proteins, proteins and polysaccharides, or proteins and DNA, play crucial roles in diverse biological processes [1,2]. In particular, the interactions between polysaccharides and proteins are key to a range of physiological and pathological processes, including blood coagulation, inflammation and tumor metastasis [3–6]. A fundamental understanding of the biophysical nature of these events, such as adhesion force, binding affinity and stability in different kinds of environments, has major applied importance [7,8]. Heparin, a highly sulfated glycosaminoglycan (GAG), is widely used as an injectable anticoagulant as well as in the form of anticoagulant coatings on various biomedical devices. Heparin is known to accelerate the inactivation of blood coagulation proteinase (thrombin) by its inhibitor antithrombin (AT) [9,10]. The mechanism of this reaction reveals a classic interplay of site-specific and site-nonspecific interactions. The first step involves AT binding to a specific five residue sequence on the polymeric chain of heparin. Thrombin binds to a remote site on the same heparin chain and then "walks" toward AT to form the ternary 'locked' complex, which results in thrombin inhibition [11–14]. For optimal operation, nature has designed heparin–thrombin interaction to be a site-nonspecific interaction [15], which enables "walking" of thrombin on the sulfated polysaccharide chain [14]. This is expected to be characterized by fast 'on' and 'off' reactions. Interestingly, the formation of the ternary complex is to be achieved under rapid blood flow conditions, which enhances the probability of thrombin dissociation and raises the possibility of inadvertent clot formation. Thus, thrombin regulation is of paramount importance and understanding the fundamentals of the heparin–thrombin interaction is critical.

To date, the binding interactions between heparin and thrombin have been studied primarily at the bulk level, using approaches such as fluorescence, affinity chromatography and surface plasmon resonance (SPR). Oshima et al. [16] showed that the interaction of thrombin with fluorescein-labeled heparin is affected by NaCl, implying that electrostatic force is the dominating factor of the interaction. Using quantitative affinity chromatography, Olson et al. [15] also demonstrated that the strong dependence of the binding on NaCl concentration was best accounted for by the electrostatic interactions of thrombin and heparin. In a study conducted via SPR, a heparin-coated surface was able to bind much more thrombin than AT III, indicating that the heparin–thrombin interaction is less specific compared to the heparin–AT III interactions [17]. However, these methods require large amounts of heparin/thrombin, and are principally applied to study the bulk scale interactions at

* Corresponding author. Tel.: +1 804 828 0587.
E-mail address: vyadavalli@vcu.edu (V.K. Yadavalli).

http://dx.doi.org/10.1016/j.bbagen.2015.01.016
0304-4165/

their steady states. They are also unable to evaluate these weak forces in varying media directly at the molecular level. On the other hand, most biological processes generally occur under non-equilibrium conditions at the molecular scale [18]. Given that the binding of thrombin and heparin might be primarily due to weak, non-covalent forces, there is a need to unravel the molecular mechanism of heparin–thrombin interaction at a fundamental level from a mechanical and dynamic perspective.

Here, we report, to the best of our knowledge, the first study of the interactions between heparin and thrombin conducted at the molecular level using atomic force microscopy (AFM)-based force spectroscopy (AFM-FS). We show the contributions of the ionic and non-ionic nature of the interaction, and the energy landscape traversed during the binding and unbinding of these molecules in the clotting cascade. Primarily devised for high resolution imaging, AFM is a powerful and widely used tool for investigating molecular scale processes. AFM-FS allows the measurement of inter- and intra-molecular interaction forces with piconewton resolution [19–21]. As the interaction forces closely depend on the loading rates exerted on the molecular complex [22,23], dynamic force spectroscopy (DFS), a subset of AFM-FS which allows collection of force data over variable loading rates, has emerged as a valuable technique for the characterization of dissociation kinetics and energy profile of the interacting molecules under varying conditions [24,25].

For force measurements using AFM-FS and DFS, the first step is to covalently immobilize each biomolecule of the pair-wise interaction on an AFM tip and a substrate, respectively. Together with different immobilization strategies, the rupture forces between the tip-bound and surface-bound molecules can then be measured in real-time, under physiological conditions, as well as under controlled microenvironments [26]. In this work, to attach the protein (thrombin) molecules to a surface and to minimize non-specific tip-surface adhesion forces, we use a well characterized mixed self-assembled monolayer (SAM) platform, wherein lysine residues on the protein surface are conjugated to NHS groups on a gold surface. However, for heparin, an additional challenge in its study lies in the development of suitable tethers for the covalent attachment of the carbohydrate. We report on the synthesis of a versatile heparin–PEG–thiol that allows facile immobilization to gold surfaces via an Au–S linkage. As we show below, heparin molecules can be modified with a poly(ethylene glycol) (PEG) containing mercapto-terminal group to enable immobilization on a gold substrate and create a functionalized surface.

The morphology of the GAG-functionalized surface was characterized via non-contact mode AFM imaging. The interaction forces of single pairs of heparin and thrombin molecules were determined in PBS buffer using AFM-FS. Control experiments were performed to measure the interaction forces between the heparin surface and bare (no attached thrombin) cantilever. The specificity of the binding interactions was confirmed via the blocking of binding sites on the thrombin molecule with free heparin. Finally, using DFS, the effect of NaCl concentration on the binding kinetics and energy landscape of the heparin and thrombin were studied. Very little is known by way of force interactions of most anticoagulation proteins (thrombin, factor Xa, factor XIa, antithrombin etc.). These experiments and findings may therefore offer a new insight into the molecular mechanism of blood (anti)coagulation under applied force or flow conditions, useful in the design and screening of cardiovascular drug candidates.

2. Materials and methods

2.1. Materials and instrumentation

(1-Mercaptoundec-11-yl) hexaethylene glycol (oligoethylene glycol (OEG) terminated thiol), HS-C_{11}-$(EG)_6$OH, and (1-mercaptohexadecanoic acid)-N-succinimidyl ester (NHS terminated thiol), HS-C_{15}COO-NHS, were purchased from Asemblon Inc. (Redmond, WA) and Nanoscience Instruments Inc. (Phoenix, AZ) respectively. Human α-thrombin was purchased from Hematologic Technologies (Essex Junction, VT). Heterofunctional polyethylene glycol (PEG): HS-PEG-NH_2 (MW 1000) was purchased from Laysan Bio (Arab, AL). Heparin sodium salt (H3393, 17,000–19,000 Da) was purchased from Sigma-Aldrich (St. Louis, MO). Phosphate-buffered saline (PBS pH 7.4) (11.9 mM phosphates, 137 mM sodium chloride and 2.7 mM potassium chloride), sodium chloride (biological, certified crystalline) and ethanol (200-proof) were purchased from Fisher Scientific. Ultrapure water (resistivity 18.2 MΩ·cm) was obtained from a MilliQ water purification system (Millipore Scientific, MA). Gold surfaces were purchased from Agilent Technologies, Inc. (Foster City, CA). Gold coated PPP-CONTCSAu cantilevers from Nanosensors (Neuchatel, Switzerland) and AC240TS cantilevers from Asylum Research (Santa Barbara, CA) were used for force measurement and imaging respectively. AFM cantilevers were cleaned using an UV/Ozone Procleaner (BioForce Nanosciences Inc. Ames, IA) before use. All AFM imaging and force spectroscopy experiments were performed using an Asylum MFP-3D atomic force microscope (Asylum Research, Santa Barbara, CA). NMR experiments were carried out on a Bruker 400 MHz NMR spectrometer (Bruker BioSpin, Woodlands, TX).

2.2. Synthesis of heparin–PEG–thiol

10 mg heparin sodium was dissolved in 1 ml formamide. 12 mg HS-PEG-NH_2 was then added and the reaction was maintained at 50 °C for 6 h. 5 mg aqueous sodium cyanoborohydride was added and incubated at 50 °C for an additional 24 h. The reaction mixture was diluted with 1 ml of water and dialyzed against 1 l of water for 48 h using a 3500 Da molecular weight cutoff dialysis membrane. The retentate was recovered and lyophilized. The freshly prepared sample was dissolved in D_2O, and further characterized by ^{1}H NMR at 400 MHz to verify the formation of the heparin–PEG–thiol. Signals, in part per million (ppm), are relative to the residual peak of the solvent (D_2O, $\delta = 4.79$ ppm).

2.3. Functionalized substrate and cantilever preparation

Gold surfaces were rinsed with ethanol several times prior to formation of the mixed thiol SAMs. Functionalized heparin substrates were prepared by a two-step method: (i) incubating the freshly cleaned gold surface in a 1 μM heparin–PEG–thiol aqueous solution for 2 h at ambient temperature, followed by rinsing with water; (ii) immersing the surface in a HS-C_{11}-$(EG)_6$OH ethanol solution overnight (16 h) followed by rinsing with ethanol. Gold coated cantilevers were cleaned in UV/ozone for 15 min. Cantilevers were functionalized by an approach as described earlier [27] — immersion in mixed thiol solution (HS-C_{11}-$(EG)_6$OH and HS-C_{15}COO-NHS) in ethanol for 16 h. Cantilevers were then rinsed with ethanol, and incubated in a 100 nM solution of thrombin in PBS buffer for 1 h at ambient temperature.

2.4. AFM imaging of surfaces and dynamic force spectroscopy

Cantilevers were cleaned using high-intensity UV light. Spring constants of functionalized cantilevers were measured prior to each experiment using the thermal fluctuation method [28]. AC240TS cantilevers ($k = \sim 2$ N/m, resonance frequency $f = 70$ kHz) were to initially characterize the heparin attached surfaces in non-contact mode. Regions containing heparin molecules were identified prior to force measurements by non-contact imaging. Subsequently, PPP-CONTCSAu cantilevers ($k \sim 0.2$ N/m, $f = 24$ kHz) functionalized with thrombin were used for measurement of interaction forces. Force–distance curves were collected in a liquid environment by moving the tip to different locations, holding it on the surface for 5 s and then retracting it in a repeated, cyclic manner. Several hundred curves were collected for each experiment at different points on the surface. The force of contact was kept at <300 pN to avoid damaging the surface heparin and to preserve the functionalized AFM tip. Force curves that showed binding events at

rupture lengths between 10 and 50 nm were selected and analyzed in IgorPro (Wavemetrics, OR). A binding probability was estimated as the ratio of the number of analyzed curves showing binding events to the total number of curves collected in each experiment. Control experiments were conducted to measure the interaction forces using bare cantilevers (PEG thiol/no attached protein) on heparin surface. Blocking experiments were performed by measuring the interaction forces in the presence of free heparin (5 μg/ml) in PBS.

By varying the loading rates of the heparin–thrombin interaction, dynamic force spectroscopy (DFS) measurements were conducted from ~10 to ~300 nN/s. The loading rate was accurately determined by estimating the speed of the cantilever at the instant of contact. At each loading rate, several hundred force–distance curves were collected and analyzed to obtain the rupture force histogram. The effect of NaCl on the binding and stability of the heparin/thrombin complex was further investigated using buffers made at varying concentrations of NaCl.

3. Results and discussion

3.1. Synthesis and characterization of heparin–PEG–thiol

To measure pair-wise interaction forces, the first step is to covalently immobilize each biomolecule on an AFM probe (cantilever) and a carefully prepared substrate [29]. The receptor and ligand are repeatedly brought in contact with one another and the molecular interaction monitored. Typically, gold-coated substrates present a wealth of possible conjugation chemistries and are widely used. In the case of thrombin, several strategies are available for covalently immobilizing the protein [30]. Here, advantage is taken of surface lysines on thrombin to attach it to a gold cantilever via an NHS linkage. On the other hand, heparin possesses unique challenges in this regard. While heparin is a negatively charged polysaccharide and could hypothetically be electrostatically immobilized to a positively charged substrate, this bond is not strong enough to prevent the molecules from being picked up by the probe during retraction [31]. It is therefore necessary to modify the heparin to enable covalent attachment, while preserving its chemical nature. Some reports have discussed the biotinylation of heparin through its un-substituted groups [32]. Here, heparin is modified using a hetero-bifunctional poly(ethylene glycol) (PEG) linker with thiol and amine end group (HS-PEG-NH_2). This creates a versatile heparin conjugate that enables covalent binding to a gold surface via an Au–S bond.

The sole reducing end of heparin was reacted with the amine group of HS-PEG-NH_2 in anhydrous formamide and the imine formed was reduced using sodium cyanoborohydride (Fig. 1A) [33]. This also allows the heparin to retain its core biochemical properties after functionalization. The heterofunctional PEG was selected for its physical and chemical inertness as well as the availability of different terminal functional groups. The PEG further acted as a spacer of controllable length between the biomolecule and the underlying substrate, allowing us to enhance bioactivity relative to direct immobilization [34]. This modification method is advantageous because of covalent attachment to the Au-substrate which makes them stable during force measurement, and also exposes the maximum number of binding sites on the heparin chain [35]. The selection of the reducing end preserves the chemical nature of the heparin. To verify this and the modification of the heparin with HS-PEG-NH_2, ^{1}H NMR was conducted. Unmodified heparin, HS-PEG-NH_2 and the product were characterized by comparison of ^{1}H NMR data (detailed peak information and spectra shown in Supplemental Fig. S1).

Heparin contains a major IdoA2S-GlcNS6S repeating disaccharide unit and minor amounts of GlcA, IdoA, GlcNAc, and GlcNS residues. ^{1}H NMR of PEG-labeled heparin showed characteristic peaks for heparin (anomeric proton of IdoA2S, and methyl of acetyl in GlcNAc), as well as the signals for PEG (2.7 ppm corresponding to $-C\underline{H}_2$-SH group and 3.7 ppm corresponding to the PEG backbone). In contrast, the newly formed linkage leads to the reduction of $NH_2C\underline{H}_2CH_2O$ signal at 3.19 ppm, and the increase of $NHC\underline{H}_2CH_2O$ signal at 2.95 ppm.

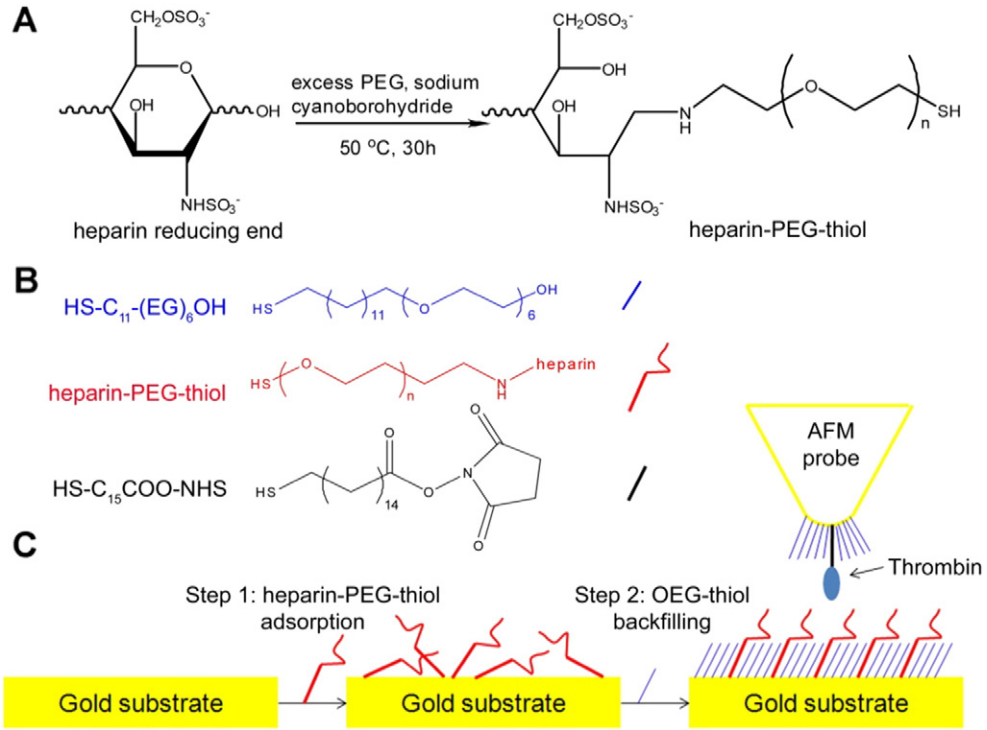

Fig. 1. (A) Schematic and structure of thiolation of heparin to form heparin–PEG–thiol. (B) Molecular structure of thiols used to form the self-assembled monolayers used in this study: HS-C_{11}-$(EG)_6$OH, heparin–PEG–thiol and HS-C_{15}COO-NHS. (C) Self-assembled monolayers formed on the gold surface and AFM probe with corresponding adsorption of heparin–PEG–thiol and thrombin on the functionalized substrates.

Attachment to amine introduces a new peak at 3.42 ppm, representing the hydrogen on the former anomeric carbon at the heparin reducing end, verifying the conjugation.

3.2. Surface modification and heparin/thrombin immobilization

For biophysical analyses between heparin and thrombin, we used a well-characterized mixed self-assembled monolayer (SAM) strategy developed by our group. This platform has been demonstrated to provide an ideal surface to attach well-separated single molecules and study single-pair interactions without the interference of non-specific adhesion [36]. Here, we used a two-step approach to form a surface with covalently immobilized heparin molecules. The heparin–PEG–thiol was first immobilized on a gold surface. This was followed by backfilling of the bare gold area with an OEG thiol ($HS\text{-}C_{11}\text{-}(EG)_6OH$) (Fig. 1B and C). The OEG thiol resists protein adhesion and nonspecific tip–surface interaction, while the sparsely distributed heparins act as reactive sites for thrombin on AFM tips. By carefully regulating the ratio of heparin–thiol to OEG thiol, the heparin density on the substrate is easily controllable.

Fig. 2A shows a non-contact AFM image of a surface with a typical concentration of immobilized heparin. The morphology of the heparin surface was homogeneous and stable after repeated AFM imaging. The 80 nm line profile across the heparin immobilized surface showed height values for the surface features that correspond well with the cross-section diameter obtained from small-angle X-ray scattering (0.9 nm) and the maximum transversal dimensions (1 nm) in the three-dimensional NMR structure of a heparin fragment [37,38]. It may be noted that the well-separated single heparins demonstrated that the "backfilling" method provided the heparin with appropriate distribution and orientation. Analyzing the length of the features from the AFM images showed that most of the heparin molecules have a length of 25–35 nm (average length of 34.1 ± 7.1 nm), consistent with the length estimated from the X-ray scattering data (32 nm contour length for a heparin with 17,800 Da and 22 nm for a flexible and mildly bent heparin with 19,000 Da) [37,39]. The different sizes of the features may result from the heterogeneous length of heparin [40]. As a control, imaging an OEG thiol surface without the heparin–thiol expectedly did not show similar features.

3.3. Measurement of heparin and thrombin interaction forces

Subsequent to the imaging, force measurements were conducted with AFM tips functionalized with thrombin on the heparin-attached surface at a loading rate of ~50 nN/s in PBS buffer. Several hundreds of force curves were collected: two sets of experiments (~300 force curves per set) were conducted on two different samples using two different tips. Of these, 19.7 ± 2.0% force curves showing a specific binding event were analyzed to construct the force distribution histogram. These curves classified as specific binding events are manifested in a cantilever deflection observed as a non-linear delayed retraction curve with a different slope as that of the contact region. The typical force–distance curve is shown in Fig. 2B. In contrast, the force curves with non-specific adhesion show a linear retraction curve with invariable slope [41]. As our group has previously demonstrated, some force curves showing a small tip-surface adhesion were also analyzed because of clearly discernible interaction events [42]. Approximately 20% of force curves with large non-specific adhesion peaks (>200 pN) were discarded. Overall, the low binding probability and percentage of non-specific adhesion events indicate that the mixed SAM platform is successfully able to modulate the orientation and density of heparin on the substrate, as well as decrease the nonspecific tip–surface interactions, critical for the accurate determination of rupture forces of individual heparin–thrombin binding pairs.

The force distribution histogram for heparin and thrombin rupture force at a loading rate of ~50 nN/s is shown in Fig. 3. The distribution of the rupture force between the heparin and thrombin shows a clear, single peak at 102.3 ± 1.3 pN. A few force curves (<4%) showed higher rupture forces, indicating that multiple molecules may be interacting. However, due to the low concentration of heparin and thrombin coupled with the mixed SAM strategy used, we can infer that most of the binding events are due to the single pair of heparin and thrombin. On increasing the concentration of heparin–PEG–thiol, the force distribution histograms showed multiple force peaks at ~100 pN, 200 pN and 300 pN (data not shown), implying that multiple pair interactions are likely to dominate with the increase of heparin density because each thrombin functionalized tip could interact with multiple heparin molecules simultaneously.

Structurally, the heparin binding site on thrombin is fairly big and almost circular. The co-crystal structure shows a hexasaccharide bound to

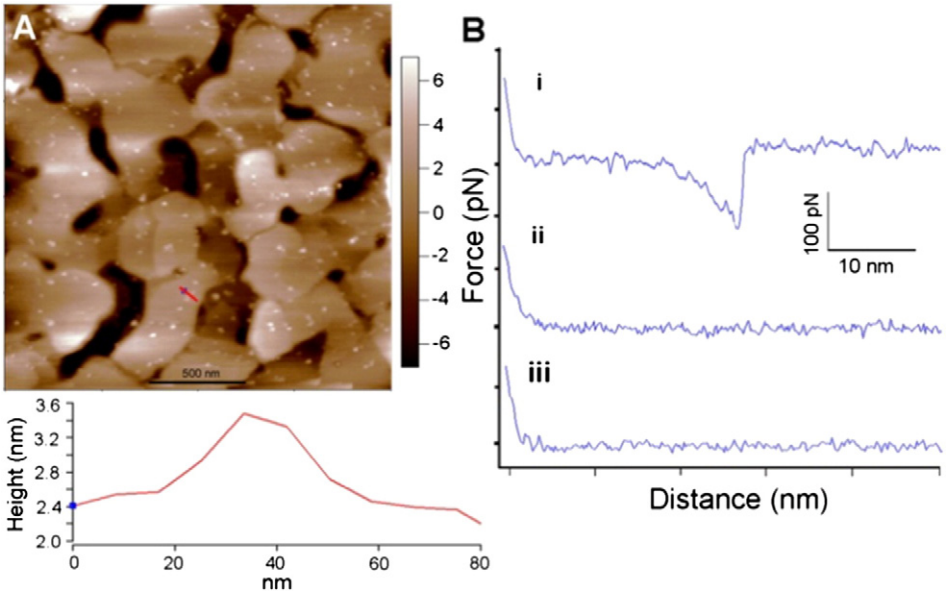

Fig. 2. (A) AFM topography images recorded in PBS of mixed SAM consisting of heparin–PEG–thiol and OH-PEG-thiol; (below) a line profile across an 80 nm section showing the height of heparin observed on the surface. (B) Typical AFM force–distance curves obtained in the experiments: (i) typical selected retract trace indicating a specific molecular recognition event; (ii) no tip-surface sticking when using the bare AFM tip (no thrombin attached); (iii) in the presence of free heparin in the PBS solution, the force drops to zero.

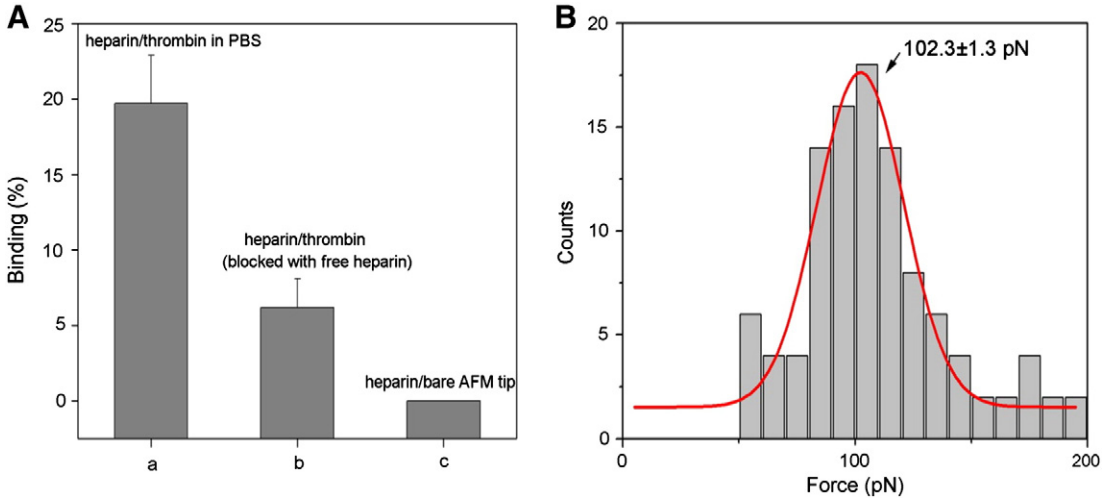

Fig. 3. (A) Comparison of binding percentages for heparin/thrombin interactions with different control experiments: a: heparin on substrate and thrombin on AFM tip; b: heparin on substrate and thrombin on AFM tip in the presence of free heparin; c: heparin on substrate and bare AFM tip (no thrombin attached). (B) Histogram showing unbinding force distributions of heparin interaction with thrombin with a Gaussian fit of the data (solid line). The Y axis represents the count number of interaction (data are from two sets of experiments, n ~ 600). The loading rate was maintained at ~50 nN/s.

thrombin but it is likely that the site of binding is longer than a hexasaccharide because key residues known to contribute to binding are spread out over distances greater than the hexasaccharide [12,39,43]. The minimal chain length that is known to bind thrombin is a trisaccharide but the typical chain length that recognizes thrombin remains unknown. In these experiments, we further tabulated the rupture distances of all collected force curves and conducted an autocorrelation analysis using a custom MATLAB program, revealing a periodicity of 5.7 nm (data shown in Supplemental Fig. S4). Thus the periodicity, corresponding to the length of heparin chain binding to thrombin, implies that the typical chain of heparin engaging thrombin is likely to be deca to dodecasaccharide (5 to 6 nm) [38]. This is also approximately the end-to-end length of anion-binding exosite II of thrombin. As heparin can bind to thrombin in multiple orientations, and because the affinities of these different modes of binding are similar, thrombin can "walk" on the heparin surface. Considering a periodicity of 5.7 nm, we may therefore posit that, at a time a discrete walk step may represent a movement of 5 to 6 nm along the chain to form the ternary locked complex.

Two different control experiments were carried out to verify that the measured forces were indeed those of the heparin/thrombin interaction. First, a bare Au-cantilever (without attached thrombin) was used to detect the heparin-attached surface. In this experiment, most of the force curves showed zero interaction (Fig. 2B) with no specific binding events detected. Second, blocking experiments were conducted by measuring the interaction forces in the presence of free heparin. The thrombin-attached tip was first incubated in heparin PBS solution for 30 min. Then force curves were collected on heparin-attached surface in the same medium. The binding probability dropped to 6.2 ± 1.9% as shown in Fig. 3. Thus we can postulate that the binding sites on the tip-attached thrombin are blocked by the free heparin in liquid. The significant decrease of binding probability of these two control experiments compared with heparin/thrombin system in PBS solution demonstrates that the observed interactions between the functionalized cantilever and the surface are likely caused by specific binding between the heparin and thrombin.

3.4. Dynamic force spectroscopy (DFS) of heparin and thrombin in PBS

It is widely acknowledged that the specific unbinding forces rely on the intrinsic interactions of molecules as well as on the loading rates. Using DFS, it is therefore possible to transform the AFM to determine useful thermodynamic and kinetic parameters [44]. By evaluating the most probable rupture forces at different loading rates, details of the dissociation dynamics of the heparin–thrombin interaction as well as the energy barriers through dissociation can be calculated. In our analysis of this system, we considered three cases — a single energy barrier, a double energy barrier model with a potential well trough between two interaction barriers, and the recently developed model by Friddle et al. that interpolates between kinetic and equilibrium regimes [44,45]. The double barrier Bell–Evans model is optimal at high loading rates and is therefore not rightly applicable to the lower loading rate regime, which contains the most interesting information in this study. Many biological systems that show "double-barriers" can be described by a single energy barrier, and the presumed "outer barrier" region simply represents near-equilibrium unbinding regime where the force does not depend on the loading rate. In our experiments as well, the rupture forces were found to be linearly dependent on the logarithm of loading rates (Fig. 4A) over the range investigated implying a single energy barrier. It is important to note that the small range of loading rates was chosen keeping in mind physiologically relevant fluid environments, such as during hemodialysis, that are relevant to the clotting cascade [46]. For the loading rate range investigated in this study, a simple linear dependence therefore precluded the need to use the model proposed by Friddle et al. [45]. However, as an internal reference, we investigated higher loading rates to 400 nN/s, wherein the force-loading rate dependence is no longer linear. Over this larger range, this model fits the data well (complete analysis shown in the Supplementary information Fig. S3). For this heparin–thrombin system however, we posit that a single barrier approach can describe the relevant interactions.

Based on this fit, kinetic parameters can be extracted using the following Bell–Evans equations described earlier [47]:

$$F = \frac{k_B T}{x_B} \ln\left(\frac{r x_B}{k_B T k_{off}}\right) \quad (1)$$

$$f_B = \frac{k_B T}{x_B} \quad \text{(slope)} \quad (2)$$

$$k_{off} = \frac{r_0}{f_B} \quad (3)$$

where F is the most probable rupture force, k_B is the Boltzmann constant, T is the absolute temperature, r is the loading rate, r_0 is the loading rate at zero force, and x_B is the distance between bound state and unbound state for the transition state, which can be calculated from the

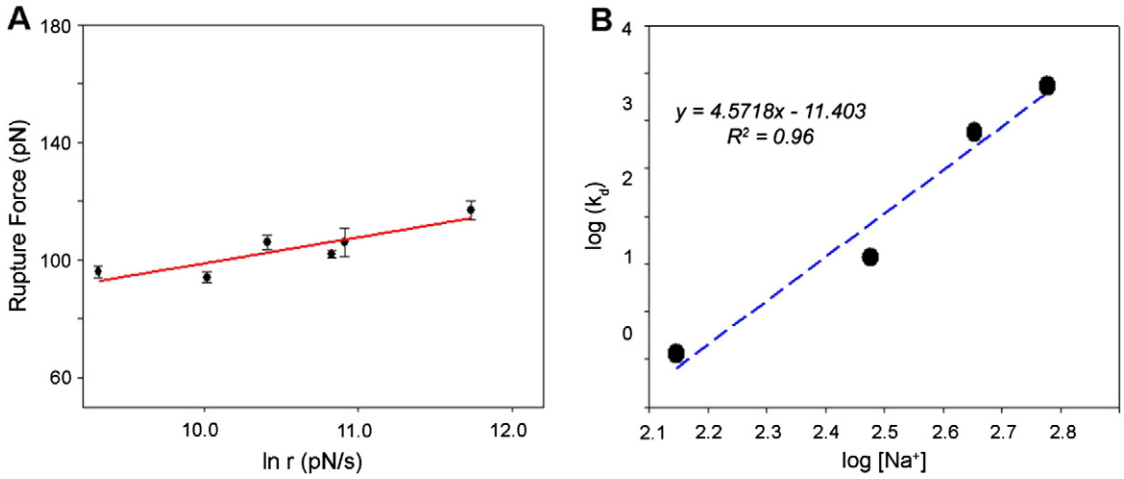

Fig. 4. Dynamic force spectra of heparin and thrombin interactions at different loading rates in PBS. (A) Fitting the data with the Bell–Evans model yields a simple linear fit. The rupture forces of the complex measured reveal the width of the energy barrier in PBS (x_B) to be 4.6 Å, while the off-rate (k_{off}) is 0.04 s^{-1}. (B) log dependence of the k_{off} with the Na^+ concentration shows a linear fit with a slope of 4.57, which corresponds very well with the earlier reported fit of 4.8 [15].

slope of fitting curve. k_{off} is the dissociation rate of bond at zero applied force, which can be calculated as the intercept of the fit. In the case of heparin and thrombin, both k_{off} and x_B are important for evaluating the susceptibility of the bond dissociation to applied force or under flow conditions [48]. Once k_{off} has been determined, the height of the energy barrier, ΔG can be deduced using the following equation according to the transition state theory [49,50]:

$$\Delta G = -k_B T \ln \frac{k_{off} h}{k_B T} \quad (4)$$

where h is Planck's constant and k_BT is the thermal energy. The linear fit to the data points in Fig. 4A indicates that the heparin–thrombin complex overcomes one energy barrier during its dissociation under applied force with a height of 32.80 k_BT. The corresponding k_{off} for the heparin–thrombin interaction in PBS was found to be 0.04 s^{-1}. The low k_{off} indicates the formation of a highly stable complex between heparin and thrombin.

3.5. Binding as a function of NaCl concentration

Finally, we investigated the binding kinetics of the heparin–thrombin interaction in the presence of salt. This served two purposes — to observe the heparin–thrombin energy landscape, and provide an internal reference for this system. Previous study has shown that NaCl has a strong influence on the interactions of heparin–thrombin and the binding of heparin and thrombin can be described by the relationship [15]:

$$\log K_{d,\ obs} = \log K_{d(\text{non-ionic})} + \alpha \log \left[Na^+\right], \quad (5)$$

where α is related to the number of Na^+ ions released upon charge-neutralization reaction between heparin and thrombin. The negatively charged sulfo/carboxyl groups on the heparin chains can form ion pairs with positively charged residues on thrombin. Initially, the repulsive energy of multiple negatively charged groups in heparin promotes the binding of Na^+ to minimize these forces. When heparin binds thrombin, the positively charged residues interact at the anionic sites to result in the entropically favorable release of Na^+ ions. However, there can also be a significant influence to the binding via H-bonding [51]. The energy of interaction therefore has contributions from the polyelectrolyte effect, H-bonding and hydrophobic interactions. To uncover the specific effect of NaCl on heparin–thrombin interaction at the molecular scale, we applied DFS to study the dissociation kinetics and energy profile under different NaCl concentrations (300 mM, 450 mM and 600 mM). The high salt concentration is used to demonstrate this polyelectrolyte effect. As previously shown in PBS (137 mM NaCl), rupture forces were acquired over a range of loading rates between ~10 nN/s and ~200 nN/s at different NaCl concentrations and plotted as a function of loading rates. It can be seen that increasing the NaCl concentration resulted in decreased rupture forces (raw data shown in Supplementary information Table S1). The strength of the heparin/thrombin complex therefore becomes weaker with an increase of salt concentration. Fitting the forces vs. loading rates reveals that the interactions are compatible with the single energy barrier model. The fitted dissociation kinetic parameters of the model are tabulated in Table 1 and the sketch of energy profile at different NaCl concentrations is shown in Fig. 5.

The force-spectroscopy results show the predicted (Eq. (5)) linear log-dependence in the off-rates vs. $[Na^+]$. The logarithm of the observed k_{off} for the heparin–thrombin interaction is directly proportional to log $[Na^+]$ in buffer (Fig. 4B). Remarkably, the linear fit of the data reveals a slope of 4.6, which is very close to the earlier reported regression fit of 4.8 obtained via fluorescence titrations [15]. This implies that 4–5 ionic interactions are involved in the heparin–thrombin interaction. It can be seen that as the $[Na^+]$ increases, the contribution of the polyelectrolyte decreases. Extrapolating this dependence indicates that the binding reflects complete contribution of the non-polyelectrolyte binding at 1.1 M salts, which is close to the ideal value of 1 M according to Eq. (1). Indeed, as observed from the energy barrier, an increase in salt concentration is manifested by a shift in the energy landscape (decrease in x_t and ΔG, Fig. 5). As the double log k_{off}–$[Na^+]$ profile is linear, it must imply that the k_{on} is invariant across the range of $[Na^+]$. This result is similar to an earlier DFS study of integrin/fibronectin interactions [52]. As shown, the energy barrier operates at lower, physiologically relevant forces, which make them more sensitive to the molecular structure or environmental changes.

The energy barrier ΔG decreases as expected with an increase in $[Na^+]$, implying that, at a sufficiently high salt concentration, the

Table 1
Dissociation kinetic parameters and energy profile of heparin/thrombin complex under different conditions.

NaCl concentration	k_{off} (s^{-1})	x_B (nm)	ΔG (k_BT)
PBS (137 mM)	0.04	0.46	32.8
300 mM	0.37	0.42	30.45
450 mM	7.6	0.28	27.42
600 mM	22.96	0.23	26.32

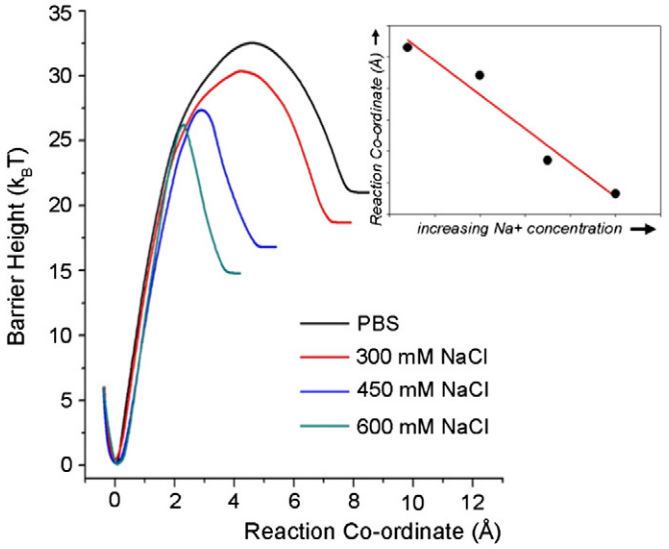

Fig. 5. Sketches of energy landscapes show intermolecular potential of the heparin/thrombin interactions in PBS with increasing NaCl concentration. The positions of energy barrier together with the height of thermal energies are derived from the linear fit of the dynamic force spectroscopy data. For example, in PBS (black), the x_β and the ΔG are calculated to be 4.6 Å and 32.8 k_BT. These parameters characterizing energy landscapes under different conditions are also summarized in Table 1. The energy landscapes showed that both the position (Inset) and the height of the interaction energy barrier shifted toward lower values with the increase in NaCl concentration.

off-rate is driven by non-ionic interaction. The energy barrier of the heparin–thrombin reaction is kinetically invisible but mechanistically significant. From a loading rate perspective, a shift to lower x_t and ΔG is also observed at faster loading rates. These results therefore show that at higher loading, the nonionic forces between heparin and thrombin, which are highly directional in comparison to ionic forces, can be expected to "orient" the thrombin molecule on the heparin chain. Once initiated and established at higher flows, electrostatic forces facilitate the movement of thrombin toward antithrombin along the heparin chain. One can predict that the initial "orientation" is such that it favors the formation of the (eventual) productive antithrombin–thrombin complex. A recent computational analysis predicts the occurrence of weak nonionic forces in heparin–thrombin interaction supporting the above conclusion [53].

This analysis revealed that the stability of the heparin/thrombin complex is suppressed by higher salt concentration. This conclusion is consistent with the theory of protein–polyelectrolyte interactions, in which the binding of the complex is reduced with increase ionic strength, due to the screening of electrostatic attractions [54]. Within this framework, the binding of thrombin to heparin in the presence of monovalent cation can be regarded as an ion exchange-type process involving the stoichiometric release of bound counter-ions from negatively charged groups on the heparin polyelectrolyte chain. The binding of thrombin to heparin is therefore not favored when the Na^+ concentration is elevated due to the unfavorable release of Na^+ ions from the polysaccharide into a salt solution [55]. Earlier molecular simulations of heparin–FX06 interaction showed that the electrostatic interaction between heparin and the positively charged FX06 residues was the main contributor for lowering the Gibbs free energy and stabilizing the complex [56]. FX06 is a peptide fragment from fibrin, and its interaction with heparin is closely related to endothelial cell adhesion, spreading and proliferation [57]. Such detailed information can typically not be extracted from bulk kinetic measurements. The single-molecule force spectroscopy study therefore uncovers the nature of the biophysical interactions and helps explains the operation of this fundamental biochemical process.

4. Conclusions

In this work, for the first time we show a molecular approach to investigate the nature of the heparin–thrombin interaction using AFM-based force spectroscopy and uncover the contributions of the electrostatic and non-ionic contributors to this interaction. As critical components of the blood coagulation cascade, it is important to elucidate these interactions. Here, we focused on developing a protein-resistant and GAG-functionalized surface for measuring interactions in different liquid environments using dynamic force spectroscopy. The versatile heparin conjugate synthesized here is a key to covalent immobilization to Au surfaces and can be widely applied to several types of interaction analyses and investigations. By changing the NaCl concentration, we further showed that the heparin–thrombin complexes are less stable with increase of NaCl concentration, implying that electrostatic components are the primary contributor to the energy landscape of the heparin/thrombin interaction. In AFM-FS, the dependence of binding on the interaction time (time of thrombin-attached tip contacting with a heparin functionalized-surface) could be used to roughly estimate the association rate constant k_{on}, whereby the dissociation constant K_{off} (k_{off}/k_{on}) could be determined [46]. Future efforts can therefore study the change in dissociation constant K_{off} with [Na^+] and further quantitatively correlate with conventional equilibrium approaches. The platform developed in this study coupled with heparin-modified tip (heparin–PEG–SH on gold coated cantilever) also shows the potential to detect interactions with multiple coagulation related proteins (including factor Xa, factor XIa and antithrombin) and elucidate molecular mechanism of blood (anti)coagulation. These insights into the heparin–thrombin interaction from a force and energy viewpoint at the single molecule scale can provide better understanding of the mechanisms of blood (anti)coagulation under applied force or flow conditions.

Transparency document

The Transparency document associated with this article can be found, in the online version.

Acknowledgments

This research was funded by grant # P01 HL107152 from the National Heart, Lung and Blood Institute (NIH/NHLBI).

Appendix A. Supplementary data

Supplementary data to this article can be found online at http://dx.doi.org/10.1016/j.bbagen.2015.01.016.

References

[1] P. Hinterdorfer, Y.F. Dufrene, Detection and localization of single molecular recognition events using atomic force microscopy, Nat. Methods 3 (2006) 347–355.
[2] C. Bustamante, Y.R. Chemla, N.R. Forde, D. Izhaky, Mechanical processes in biochemistry, Annu. Rev. Biochem. 73 (2004) 705–748.
[3] C.R. Bertozzi, L.L. Kiessling, Chemical glycobiology, Science 291 (2001) 2357–2364.
[4] M.P. Sheetz, Cell control by membrane–cytoskeleton adhesion, Nat. Rev. Mol. Cell Biol. 2 (2001) 392–396.
[5] H. Lis, N. Sharon, Lectins: carbohydrate-specific proteins that mediate cellular recognition, Chem. Rev. 98 (1998) 637–674.
[6] I. Bjork, U. Lindahl, Mechanism of the anticoagulant action of heparin, Mol. Cell. Biochem. 48 (1982) 161–182.
[7] R. Jelinek, S. Kolusheva, Carbohydrate biosensors, Chem. Rev. 104 (2004) 5987–6015.
[8] C. Ray, S.L. Guo, J. Brown, N. Li, B.B. Akhremitchev, Kinetic parameters from detection probability in single molecule force spectroscopy, Langmuir 26 (2010) 11951–11957.
[9] J.I. Weitz, Low-molecular-weight heparins, N. Engl. J. Med. 337 (1997) 688–698.
[10] R.M. Maaroufi, M. Jozefowicz, T. TaponBretaudiere, A.M. Fischer, Mechanism of thrombin inhibition by antithrombin and heparin cofactor II in the presence of heparin, Biomaterials 18 (1997) 203–211.
[11] V.J. Streusand, I. Bjork, P.G.W. Gettins, M. Petitou, S.T. Olson, Mechanism of acceleration of antithrombin–proteinase reactions by low-affinity heparin, J. Biol. Chem. 270 (1995) 9043–9051.

[12] W. Li, D.J.D. Johnson, C.T. Esmon, J.A. Huntington, Structure of the antithrombin–thrombin–heparin ternary complex reveals the antithrombotic mechanism of heparin, Nat. Struct. Mol. Biol. 11 (2004) 857–862.
[13] A. Danielsson, E. Raub, U. Lindahl, I. Bjork, Role of ternary complexes, in which heparin binds both antithrombin and proteinase, in the acceleration of the reactions between antithrombin and thrombin or factor Xa, J. Biol. Chem. 261 (1986) 5467–5473.
[14] U.R. Desai, New antithrombin based anticoagulants, Med. Res. Rev. 24 (2004) 151–181.
[15] S.T. Olson, H.R. Halvorson, I. Bjork, Quantitative characterization of the thrombin–heparin interaction. Discrimination between specific and nonspecific binding models, J. Biol. Chem. 266 (1991) 6342–6352.
[16] G. Oshima, H. Uchiyama, K. Nagasawa, Effect of NaCl on the association of thrombin with heparin, Biopolymers 25 (1986) 527–537.
[17] C.J. vanDelden, J.P. Lens, R.P.H. Kooyman, G.H.M. Engbers, J. Feijen, Heparinization of gas plasma-modified polystyrene surfaces and the interactions of these surfaces with proteins studied with surface plasmon resonance, Biomaterials 18 (1997) 845–852.
[18] X.J. Zhang, V.K. Yadavalli, Molecular interaction studies of vascular endothelial growth factor with RNA aptamers, Analyst 135 (2010) 2014–2021.
[19] H. Clausen-Schaumann, M. Seitz, R. Krautbauer, H.E. Gaub, Force spectroscopy with single bio-molecules, Curr. Opin. Chem. Biol. 4 (2000) 524–530.
[20] Y. Seo, W. Jhe, Atomic force microscopy and spectroscopy, Rep. Prog. Phys. 71 (2008) 1–23.
[21] F.J. Giessibl, C.F. Quate, Exploring the nanoworld with atomic force microscopy, Phys. Today 59 (2006) 44–50.
[22] E.A. Evans, D.A. Calderwood, Forces and bond dynamics in cell adhesion, Science 316 (2007) 1148–1153.
[23] Y-S. Lo, Y-J. Zhu, T.P. Beebe, Loading-rate dependence of individual ligand-receptor bond-rupture forces studied by atomic force microscopy, Langmuir 17 (12) (2001) 3741–3748.
[24] E. Evans, Probing the relation between force – lifetime – and chemistry in single molecular bonds, Annu. Rev. Biophys. Biomol. Struct. 30 (2001) 105–128.
[25] C. Hyeon, D. Thirumalai, Multiple barriers in forced rupture of protein complexes, J. Chem. Phys. 137 (2012).
[26] L.W. Francis, P.D. Lewis, C.J. Wright, R.S. Conlan, Atomic force microscopy comes of age, Biol. Cell. 102 (2010) 133–143.
[27] V.K. Yadavalli, J.G. Forbes, K. Wang, Functionalized self-assembled monolayers on ultraflat gold as platforms for single molecule force spectroscopy and imaging, Langmuir 22 (2006) 6969–6976.
[28] J.L. Hutter, J. Bechhoefer, Calibration of atomic force microscope tips, Rev. Sci. Instrum. 64 (1993) 1868–1873.
[29] K.C. Neuman, A. Nagy, Single-molecule force spectroscopy: optical tweezers, magnetic tweezers and atomic force microscopy, Nat. Methods 5 (2008) 491–505.
[30] F. Rusmini, Z.Y. Zhong, J. Feijen, Protein immobilization strategies for protein biochips, Biomacromolecules 8 (2007) 1775–1789.
[31] P. Wagner, Immobilization strategies for biological scanning probe microscopy, FEBS Lett. 430 (1998) 112–115.
[32] H.N. Yu, E.M. Munoz, R.E. Edens, R.J. Linhardt, Kinetic studies on the interactions of heparin and complement proteins using surface plasmon resonance, Biochim. Biophys. Acta 1726 (2005) 168–176.
[33] B. Pasche, K. Kodama, O. Larm, P. Olsson, J. Swedenborg, Thrombin inactivation on surfaces with covalently bonded heparin, Thromb. Res. 44 (1986) 739–748.
[34] H. Chen, Y. Chen, H. Sheardown, M.A. Brook, Immobilization of heparin on a silicone surface through a heterobifunctional PEG spacer, Biomaterials 26 (2005) 7418–7424.
[35] V.D. Nadkarni, A. Pervin, R.J. Linhardt, Directional immobilization of heparin onto beaded supports, Anal. Biochem. 222 (1994) 59–67.
[36] X.J. Zhang, V.K. Yadavalli, Surface immobilization of DNA aptamers for biosensing and protein interaction analysis, Biosens. Bioelectron. 26 (2011) 3142–3147.
[37] G. Pavlov, S. Finet, K. Tatarenko, E. Korneeva, C. Ebel, Conformation of heparin studied with macromolecular hydrodynamic methods and X-ray scattering, Eur. Biophys. J. Biophys. Lett. 32 (2003) 437–449.
[38] B. Mulloy, M.J. Forster, C. Jones, D.B. Davies, Nmr and molecular-modeling studies of the solution conformation of heparin, Biochem. J. 293 (1993) 849–858.
[39] S. Khan, J. Gor, B. Mulloy, S.J. Perkins, Semi-rigid solution structures of heparin by constrained X-ray scattering modelling: new insight into heparin–protein complexes, J. Mol. Biol. 395 (2010) 504–521.
[40] F.J. Spinelli, K.L. Kiick, E.M. Furst, The role of heparin self-association in the gelation of heparin-functionalized polymers, Biomaterials 29 (2008) 1299–1306.
[41] C.K. Lee, Y.M. Wang, L.S. Huang, S.M. Lin, Atomic force microscopy: determination of unbinding force, off rate and energy barrier for protein–ligand interaction, Micron 38 (2007) 446–461.
[42] X.J. Zhang, V.K. Yadavalli, Functionalized self-assembled monolayers for measuring single molecule lectin carbohydrate interactions, Anal. Chim. Acta. 649 (2009) 1–7.
[43] W.J. Carter, E. Cama, J.A. Huntington, Crystal structure of thrombin bound to heparin, J. Biol. Chem. 280 (2005) 2745–2749.
[44] A. Noy, R.W. Friddle, Practical single molecule force spectroscopy: how to determine fundamental thermodynamic parameters of intermolecular bonds with an atomic force microscope, Methods 60 (2013) 142–150.
[45] R.W. Friddle, A. Noy, J.J. De Yoreo, Interpreting the widespread nonlinear force spectra of intermolecular bonds, Proc. Natl. Acad. Sci. U. S. A. 109 (2012) 13573–13578.
[46] M. Allon, M.L. Robbin, Increasing arteriovenous fistulas in hemodialysis patients: problems and solutions, Kidney Int. 62 (2002) 1109–1124.
[47] E. Evans, K. Ritchie, Dynamic strength of molecular adhesion bonds, Biophys. J. 72 (1997) 1541–1555.
[48] R. Alon, S.Q. Chen, K.D. Puri, E.B. Finger, T.A. Springer, The kinetics of L-selectin tethers and the mechanics of selectin-mediated rolling, J. Cell Biol. 138 (1997) 1169–1180.
[49] T. Strunz, K. Oroszlan, I. Schumakovitch, H.J. Guntherodt, M. Hegner, Model energy landscapes and the force-induced dissociation of ligand–receptor bonds, Biophys. J. 79 (2000) 1206–1212.
[50] Z.J. Lv, J.H. Wang, G.P. Chen, Exploring the energy profile of human IgG/Rat anti-human IgG interactions by dynamic force spectroscopy, Protein J. 31 (2012) 425–431.
[51] I. Capila, R.J. Linhardt, Heparin– protein interactions, Angew. Chem. Int. Ed. 41 (2002) 391–412.
[52] F.Y. Li, S.D. Redick, H.P. Erickson, V.T. Moy, Force measurements of the alpha(5) beta(1) integrin–fibronectin interaction, Biophys. J. 84 (2003) 1252–1262.
[53] P.D. Mosier, C. Krishnasamy, G.E. Kellogg, U.R. Desai, On the specificity of heparin/heparan sulfate binding to proteins. anion-binding sites on antithrombin and thrombin are fundamentally different, PLoS One 7 (2012).
[54] E. Seyrek, P.L. Dubin, C. Tribet, E.A. Gamble, Ionic strength dependence of protein–polyelectrolyte interactions, Biomacromolecules 4 (2003) 273–282.
[55] G.S. Manning, Molecular theory of polyelectrolyte solutions with applications to electrostatic properties of polynucleotides, Q. Rev. Biophys. 11 (1978) 179–246.
[56] C.L. Guo, B. Wang, L.C. Wang, B.Q. Xu, Structural basis of single molecular heparin–FX06 interaction revealed by SPM measurements and molecular simulations, Chem. Commun. 48 (2012) 12222–12224.
[57] T.M. Odrljin, C.W. Francis, L.A. Sporn, L.A. Bunce, V.J. Marder, P.J. SimpsonHaidaris, Heparin-binding domain of fibrin mediates its binding to endothelial cells, Arterioscler. Thromb. Vasc. Biol. 16 (1996) 1544–1551.